

NUMERICAL ANALYSIS OF METAL FOAMS SUBMITTED TO DYNAMICAL LOADING

Luiz A. B da Cunda^a, Branca F. Oliveira^b and Guillermo J. Creus^c

^a*Escola de Engenharia, Universidade Federal do Rio Grande, Av. Itália km 08, Campus Carreiros, 96201-900, Rio Grande, RS, Brazil, luizcunda@furg.br*

^b*Federal University of Rio Grande do Sul, Av. Osvaldo Aranha, 99 - 408, 90035-190, Porto Alegre, RS, Brazil, branca@ufrgs.br*

^c*Federal University of Rio Grande do Sul, Av. Bento Gonçalves, 9500, 91509-900 Porto Alegre, RS, Brazil, creus@ufrgs.br*

Keywords: Metallic foams, Plasticity, Damage, Finite Elements, Dynamic Analysis.

Abstract. Metallic foams provide low density, high specific stiffness, high energy absorption and good damping and are thus interesting alternatives for structural applications. Impact energy is dissipated through cell bending, buckling or fracture. On the other hand, results of the strain-rate and inertia effects during dynamic deformation of cellular metals are apparently conflicting. A better understanding is found in studies that show that the relative importance of the strain-rate and inertia effects depends on the impact velocity and the geometry of the structure, but still no particular formulation is generally accepted. In the present paper, computational dynamical analyses of Representative Volume Elements (RVE) of Metallic Hollow Sphere Structures (MHSS) and RVE sets are performed considering various geometries, material properties and loading rates.

1 INTRODUCTION

Metallic foams and cellular metals are materials composed by a metallic matrix with internal voids (Gibson et al., 1997; Ashby et al., 2000). They show mechanical behaviour and physical properties that strongly differ from those of solid materials and offer interesting combinations of properties as, for example, high stiffness combined with low specific weight, or permeability to gas flow combined with high thermal conductivity. Important characteristics of metallic foams are their excellent ability for energy absorption (Nemat-Nasser et al., 2007) and high specific stiffness (Fiedler, 2007; Öchsner et al., 2003). The combination of such mechanical properties with excellent sound and heat isolation opens for these materials a wide field of potential engineering applications.

The schematic stress-strain curve of a metallic foam in compression is presented in Fig. 1 that shows a large area in the plateau region corresponding to high energy absorption at constant stress.

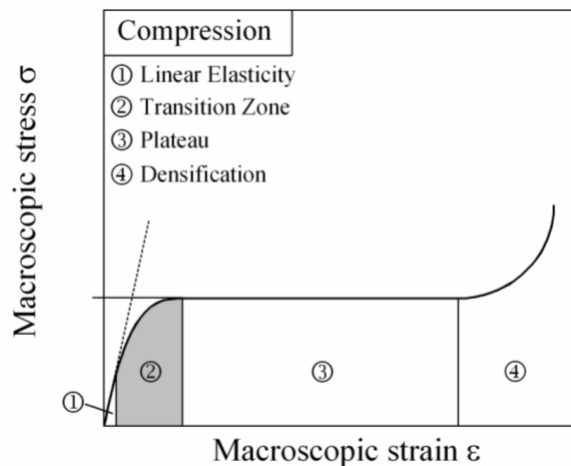


Figure 1: Stress-strain curve for a metallic foam showing large capacity of energy absorption at constant stress (Öchsner et al., 2003)

The high-strain-rate stress–strain response of metallic foams has received increased attention in recent years because of their potential for energy absorption during deformation under impact. A better understanding of the deformation mechanisms present in these materials would enable designers to more fully utilize their energy absorbing characteristics.

A good energy-absorbing material needs to dissipate the kinetic energy of the impact, while keeping the force on it below some limit. In the case of a car, it is important to assure that a safe deceleration rate is applied on the occupants. In Cardoso and Oliveira (2010) finite element simulations for the concept vehicle “Sabiá 5” (Fig. 2) using ABAQUS are given and the results from a crash test numerically performed are presented. The “Sabiás” are hyper-economic vehicles created to compete in an energy economy racing circuit (Shell Eco-Marathon). The simulations shown were generated in association with Smarttech – SP and the vehicle was impacted against a stiff barrier at a speed of 50 km/h.

Figure 3 shows a comparison of the kinetic energy absorbed in the crash test simulation for three optional chassis models for the vehicle: whole aluminium, whole metal foam and sandwich panel with metal foam filling.

Figure 4 shows the plastic dissipation for the three chassis models and figures 5 and 6 show the equivalent plastic deformation for the sandwich composition model and the metal foam model, respectively.

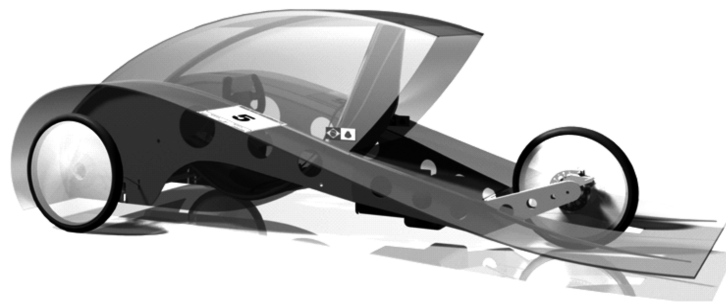


Figure 2: Vehicle Sabiá 5 (Cardoso and Oliveira, 2010)

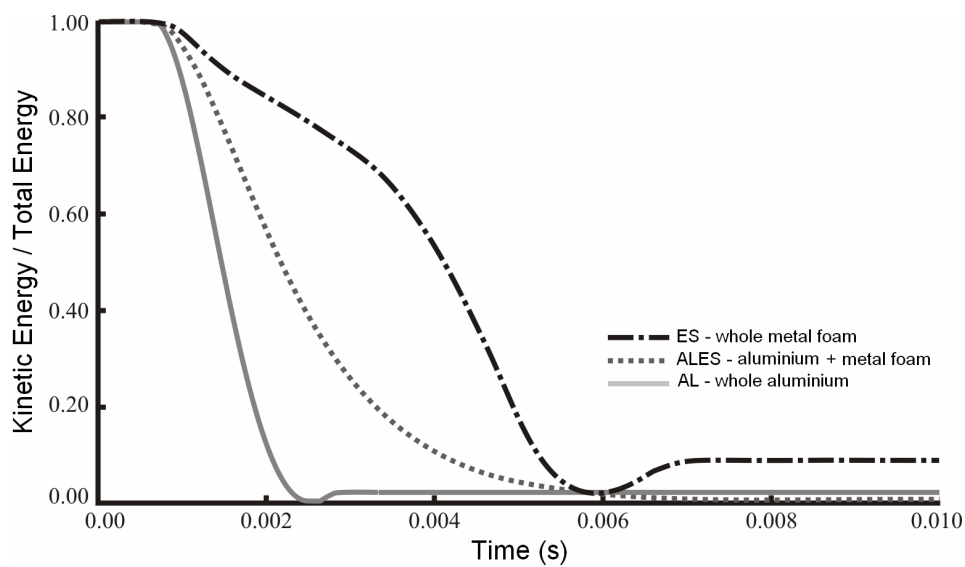


Figure 3: Comparison of the kinetic energy absorption for the three types of material (Cardoso and Oliveira, 2010)

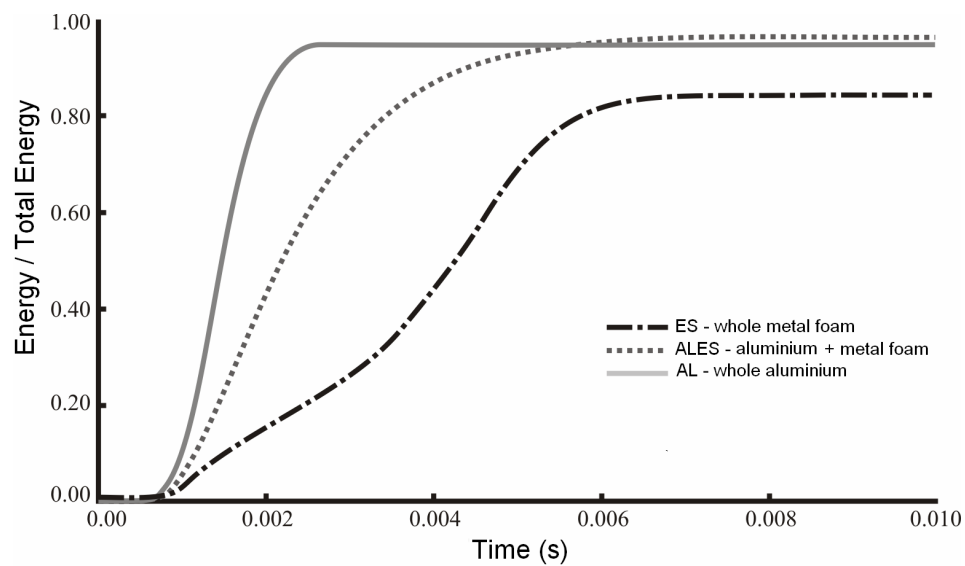


Figure 4: Comparison of the plastic energy dissipation for the three types of material (Cardoso and Oliveira, 2010)

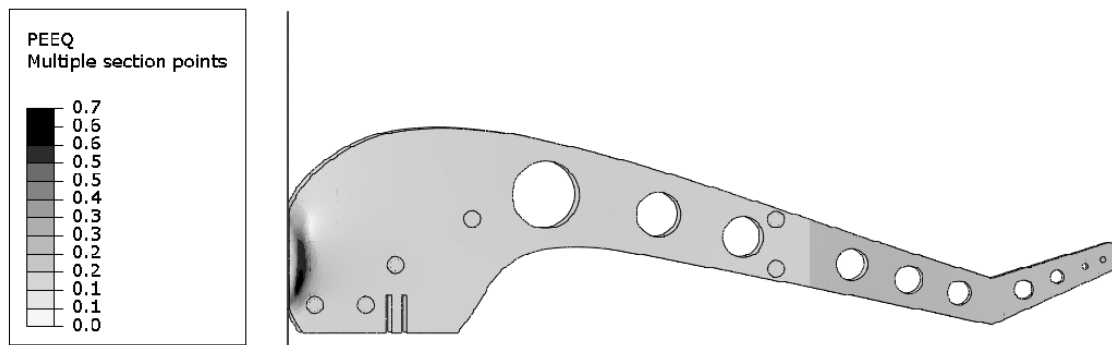


Figure 5: Crash test equivalent plastic deformation for the model with aluminium sides and metal foam filling (sandwich) (Cardoso and Oliveira, 2010)

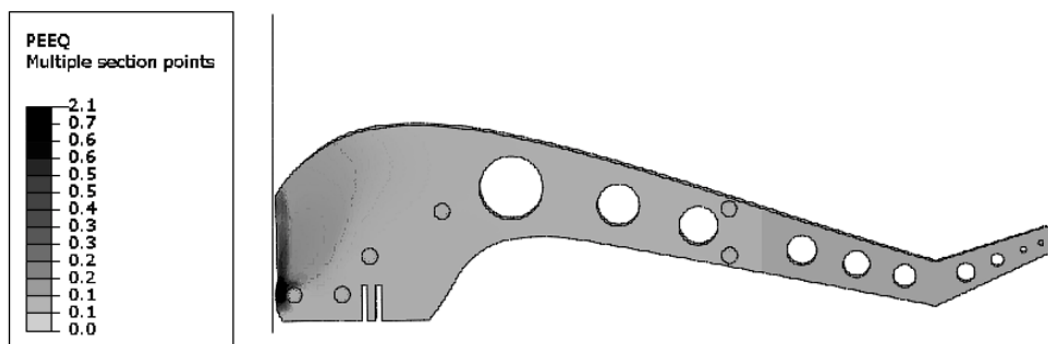


Figure 6: Crash test equivalent plastic deformation for the metal foam model (Cardoso and Oliveira, 2010)

The metal foam model suffered the greatest plastic deformation; however, this model had the slowest kinetic energy absorption, taking three times longer to reach the same level as the whole aluminium model.

In the present paper, Abaqus (in both Standard and Explicit versions) was employed to analyze the dynamic compression behavior of Metallic Hollow Sphere Structures (MHSS), studying the deformation of a unit cell as well as of cells assemblies under different impact velocities. MHSS differ from traditional open or closed-cell metal foams because of their more homogeneous structure (Fig. 7).

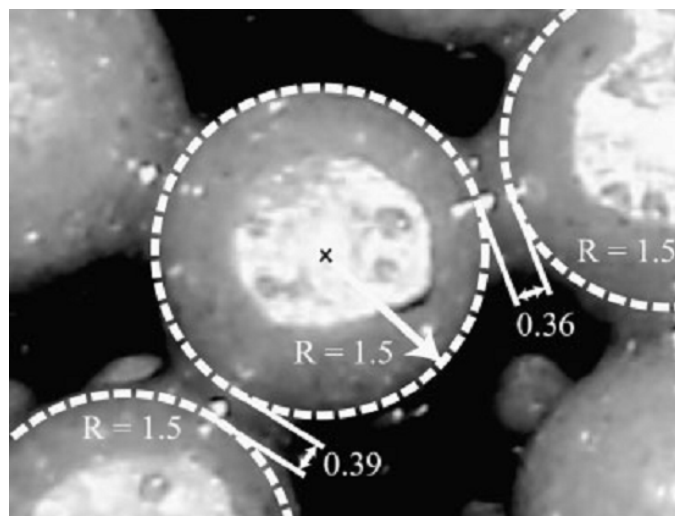


Figure 7: MHSS morphology indicating some typical dimensions in mm (Fiedler, 2007)

The authors have already performed experimental and numerical studies (Oliveira et al., 2008; Oliveira et al., 2009a; Oliveira et al., 2009b) on the quasi-static behavior of cellular metals and MHSS (Fig. 8). The analysis of a single sphere behavior showed that damage has little effect on the load-displacement relation, which depends on boundary conditions. This dependence is confirmed by the results (Fig. 8, Oliveira et al., 2009b) with a RVE and a 5x5 cells structure (a square layer with 5 cells in each direction). The comparison of experimental and numerical results showed a fairly good approximation. The jumps in the numerical curve, not observed in the experiments, are probably due to random properties that smoothes up such details.

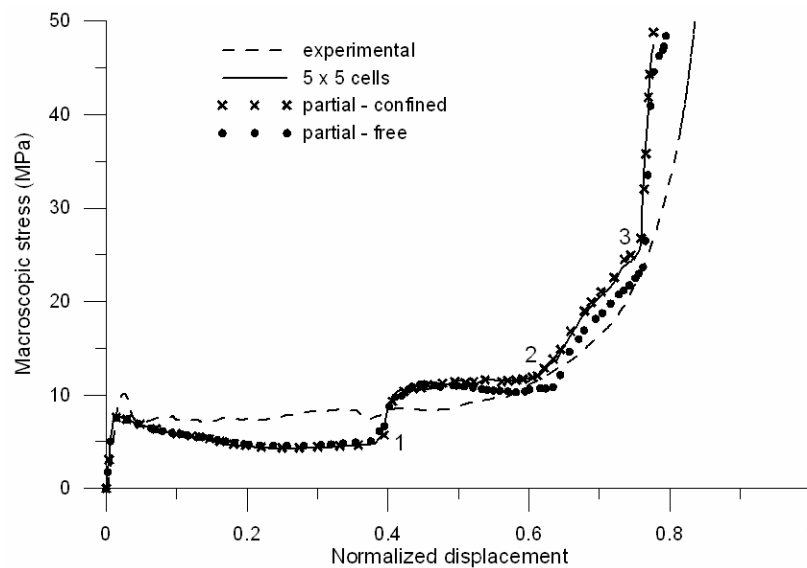


Figure 8: Macroscopic stress versus normalized displacement plots considering a confined RVE, a free RVE and the 5x5 cells model (Oliveira et al., 2009b)

The content of the present paper is as follows. In section 2 it is presented a review on some works related with the present study is presented. Section 3 shows the methods and materials used. Section 4 presents and discusses the finite element simulations performed and section 5 gives the conclusions and final comments.

2 REVIEW AND BACKGROUND

Metal foams can undergo large compressive deformations and absorb considerable amounts of energy. The energy is dissipated through the cell bending, buckling or fracture and stress is fairly constant in the stress-strain curve plateau. Thus, for a given amount of dissipated energy, a foam specimen always shows a maximum force lower than that corresponding to a solid specimen of the base material from which the foam is derived.

On the other hand, the mechanical behavior of metal foams, particularly under dynamic loading is still not well understood. Important questions to be answered are:

1. Dependence of the higher values of stress (peak and plateau values) on impact velocity;
2. Dependence of the above stresses on foam topology and base material;
3. Analytical bases for approximate or numerical calculations.

The available experimental research shows desirable properties but not well established quantitative results. For example, in Balch et al. (2005), results for syntactic foams fabricated

by liquid metal infiltration of commercially pure 7075 aluminium into preforms of hollow ceramic microspheres are given. The foams exhibited peak strengths during dynamic loading exceeding in 10–30% the corresponding quasi-static value, with strain rate sensitivities similar to those of aluminium–matrix composite materials. X-ray tomographic investigation was used to reveal differences in deformation modes. The foams displayed pronounced energy-absorbing capabilities, suggesting potential in packaging applications and impact protection.

In Cady et al. (2009), the compressive constitutive behavior of a closed-cell aluminum foam (ALPORAS) was evaluated under static and dynamic loading conditions as a function of temperature. A small change in the stress-strain behavior as a function of strain rate was measured. The deformation behavior of the Al-foam was found to be strongly temperature dependent under both quasi-static and dynamic loading.

In Montanini (2005), the structural performance of aluminium alloy foams was investigated under both static and dynamic compressive loads. Three foam typologies (M-Pore, Cymat, Schunk) in a wide range of densities (from 0.14 to 0.75 g/cm³), made by means of different processes (melt gas injection, powder metallurgy, investment casting) were analyzed to assess their strain rate sensitivity and energy absorption capability and to point out the correlation between the mechanical behavior and the physical and geometrical properties of the foam. Impact tests showed that the dependence of the plateau stress on the strain rate can be considered negligible for M-Pore and Cymat foams while it is quite remarkable for Schunk foams. Moreover, it was found that the peak stress of Cymat foams has a quite large sensitivity on the loading rate. The review of other experimental reports on dynamic deformation of cellular metals also shows results apparently conflicting (Paul and Ramamurty, 2000; Mukai et al., 2006; Dannemann and Lankford, 2000; Deshpande and Fleck, 2000; Han et al., 2005; Zhao et al., 2005).

Four causes have been proposed for the rate sensitivity of metallic cellular materials:

1. the pressure of the air trapped in the cells;
2. the rate sensitivity of the base materials;
3. the shock enhancement;
4. the micro-inertia effect.

Theoretical calculations by Zhao et al. (2005) seem to show that the effect of entrapped air would represent a very small contribution in the case of metallic foams.

As for the macroscopic rate sensitivity of the cellular materials, it depends on the rate sensitivity of the base materials. Deshpande and Fleck (2000) found that these two rate sensitivities are of the same order of magnitude. On the other hand, such influence cannot explain all the observed macroscopic rate sensitivity of aluminium foams because the rate sensitivity of aluminium is proved to be very small (Lindholm et al. (1971).

Reid and Peng (1997) reported the strength enhancement by the formation of shock waves which may happen at high impact speed (about 50 m/s). The basic idea is the possible formation of a unique shock front because the behaviour of cellular materials in their densification part is a concave function. Analytical (Harrigan et al., 2010) and experimental investigations (Zhao et al., 2005) seems to indicate that neither this effect can explain the rate effect on foams.

Thus, the remaining causes are base material rate-dependency (for some materials) and microinertia. Microinertia effects may include several components, among them those related to dynamic buckling, where the lateral inertia under impact increases strength because inertia increases the resistance to bending. If the load on a column is applied suddenly and then released, the column can sustain a load much higher than its quasi-static (slowly applied)

buckling load. This can happen, for example, in a long, unsupported column (rod) used as a drop hammer. The duration of compression at the impact end is the time required for a stress wave to travel up the rod to the other (free) end and back down as a relief wave. Maximum buckling occurs near the impact end at a wavelength much shorter than the length of the rod, at a stress many times the buckling stress if the rod were a statically-loaded column (Lindberg, 2003). Lindberg (2003) and Lee et al. (2006) study the dynamic elasto-plastic buckling of simple models, and show that the relative importance of the strain-rate and inertia effects depends on the impact velocity and the geometry of the structure. Calladine and English (1984), showed that type II structures (Fig. 9) (i.e. structures which have a falling quasi-static load-deflection curve, as metal foams after the peak load and before compaction) display more strongly strain-rate and inertia effects under dynamic loading conditions than type I structures (structures with monotonically increasing quasi-static load-deflection curves). Tam and Calladine (1991) conducted further, more detailed experiments on type II structures and pointed out that inertia is the dominant factor in the first phase (their pure compression phase) of the dynamic response to impact, whilst, in contrast, the second phase, in which energy is dissipated by plastic bending, is more sensitive to strain-rate effects.

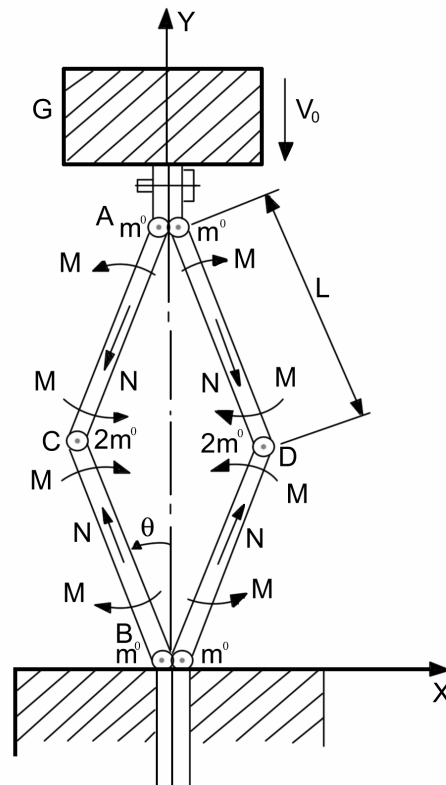


Figure 9: A structural model for the analysis of type II structures

In Su et al. (1995) a structural model which consists of four compressible elastic-plastic bars connected by four elastic-plastic "hinges" of finite length (Fig. 9) was proposed and its dynamic behavior under impact loading was analyzed in detail. The analysis shows that inertia appears to be the dominant factor in the entire deformation process and that strain-rate enhances the load-carrying capacity of these types of structures during their entire dynamic deformation.

In another important work (Lee et al., 2006), the quasi-static and dynamic compressive behavior of pyramidal truss cores made of stainless steel were investigated using a

combination of numerical and experimental techniques. Quasi-static tests were performed using a miniature loading frame. A Kolsky bar apparatus was used to investigate intermediate deformation rates and high deformation rates were examined using a light gas gun. A finite element model was used for simulations intended to understand the roles of material strain rate hardening and structural micro-inertia. Comparison of force-deformation histories under quasi-static and low deformation rates revealed a moderate micro-inertia effect as manifested by a small increase in peak compressive stress, as shown in Fig. 10. At high deformation rates, a major increase in peak compressive stress was observed. In this case, the inertia associated to the bending and buckling of truss struts played a significant role.

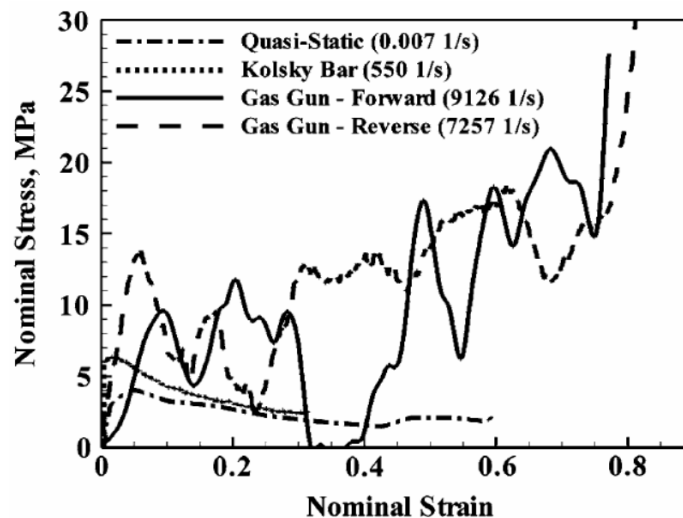


Figure 10: Stress-strain curves of pyramidal truss core being crushed at different strain rates (Lee et al., 2006)

Karagiozova and Jones (2000), that studied the dynamic elastic-plastic buckling of cylindrical shells, showed that the buckling phenomenon is governed by the whole complex of loading parameters, boundary conditions and geometrical characteristics of the specimens, so that the interaction between all impact parameters should be considered in any particular case.

It is a common computational practice (i. e. Nemat-Nasser et al., 2007) to model micro-heterogeneous materials as homogenous solids, describing the averaged motion and ignoring the local motion of RVE's. This representation may be adequate for low rates of loading, but for high rates of loading, the inertia effects associated with local motion may become significant.

The aim of our research (of which the present work represents an initial part) is to study the dynamical behavior of MHSS by means of detailed computational analyses that take account of the microstructure, using cells and cell aggregates, and studying separately the effects of material rate sensitivity, inertia and wave propagation.

3 MATERIALS AND METHODS

Representative cells (RVE) and small cell aggregates were used in order to keep computational time under control. The models used in the numerical simulation of the MHSS behavior were made to fit the global density for the set resin-metal of 0.6 g/cm^3 . The metal spheres have an external radius of 1.5 mm and the resin thickness between spheres is 0.36 mm, according the structure of the specimen of MHSS, shown in Fig 6. Three thickness values are employed: 0.0575 mm, 0.115 mm and 0.23 mm. The boundary conditions on the

vertical faces reproduce symmetry conditions on the left face and periodic boundary condition on the right face, maintaining the right face plane and vertical, but allowing horizontal displacements (Fig. 11), in order to represent the average behavior of the foam, when a vertical displacement is applied to the top side and the vertical faces must continue vertical while the distance between them may change.

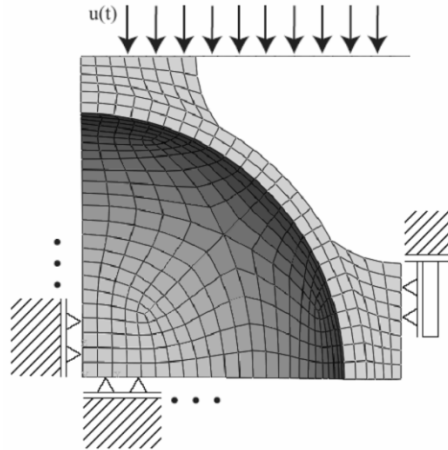


Figure 11: Finite element mesh and boundary conditions employed

Materials constants used were elastic modulus $E = 110$ GPa, Poisson's ratio $\nu = 0.30$, initial yield stress $\sigma_y^0 = 300$ MPa and density $\rho = 6.95$ g/cm³ for the metal of the sphere and $E = 2.46$ GPa, $\nu = 0.34$, compression yield stress $\sigma_y^{0,c} = 113$ MPa and density $\rho = 1.13$ g/cm³ for the resin. Both the metal sphere and the matrix were modeled as elastoplastic. Damage was considered only for the metallic spheres using the Gurson damage model (Gurson, 1977; Tvergaard, 1981; Tvergaard, 1982; Koplik and Needleman, 1988). To consider rate-dependency effects a power law is employed

$$\dot{\epsilon}^p = A \left(\frac{\bar{\sigma}}{\sigma_y} - 1 \right)^p \quad (1)$$

with $A = 40$ and $p = 5$. These values were chosen close to the maxima adequate for the spheres material.

In addition to the unit cells, columns formed by up to 5 cells stacked together were analyzed to determine the advance of the compressive shock wave (see Figs. 17 and 18).

4 FINITE ELEMENT SIMULATIONS

Numerical analyses were performed using Abaqus/Standard and Abaqus/Explicit for static and dynamic simulations respectively, with automatic time increments size in a geometrically nonlinear context. 3D, eight node linear isoparametric elements with full reduced integration were used. The mesh was determined through previous convergence tests. Sliding contact was assumed.

Results are shown as macroscopic stress (defined as the ratio between the sum of the reaction forces in the loading direction and the square surface corresponding to the projection of the undeformed sphere radius onto a plane) versus normalized displacement (defined as the relation between the imposed displacement to the top plane and the original height). The numerical results presented correspond to quasi-static loading and to dynamic loading for impact velocities of 0.14, 1.39, 2.78 and 13.89 m/s.

It must be noticed, that in the case of dynamic (as opposed to quasi-static) loading, the value of the load depends on whether it is measured at the top or at the base of the cell, as shown in Figs. 12 to 15.

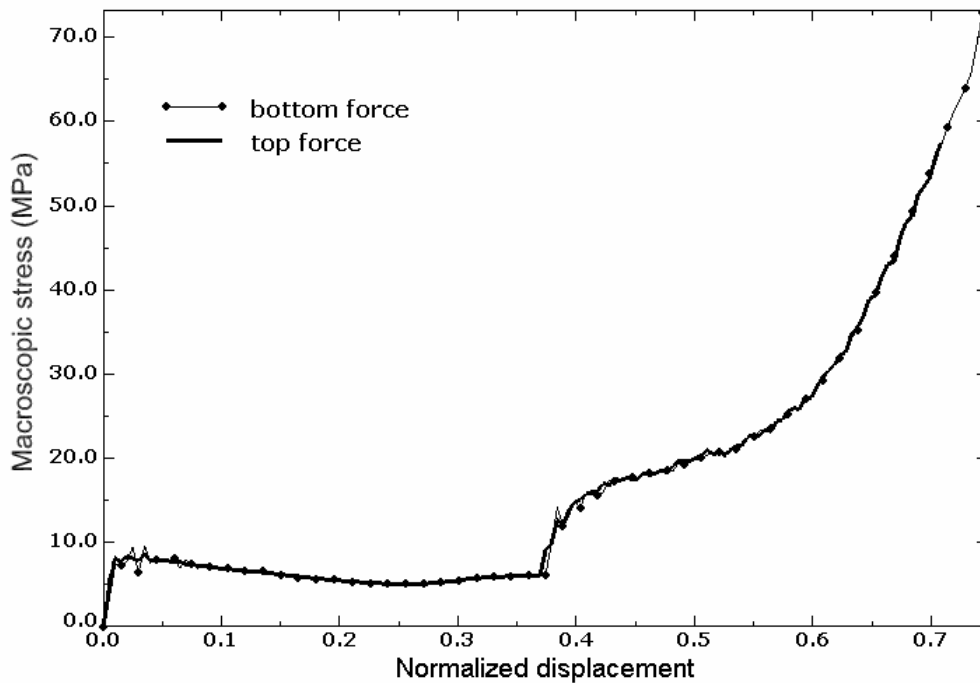


Figure 12: Macroscopic stress obtained with a velocity of 0.28 m/s

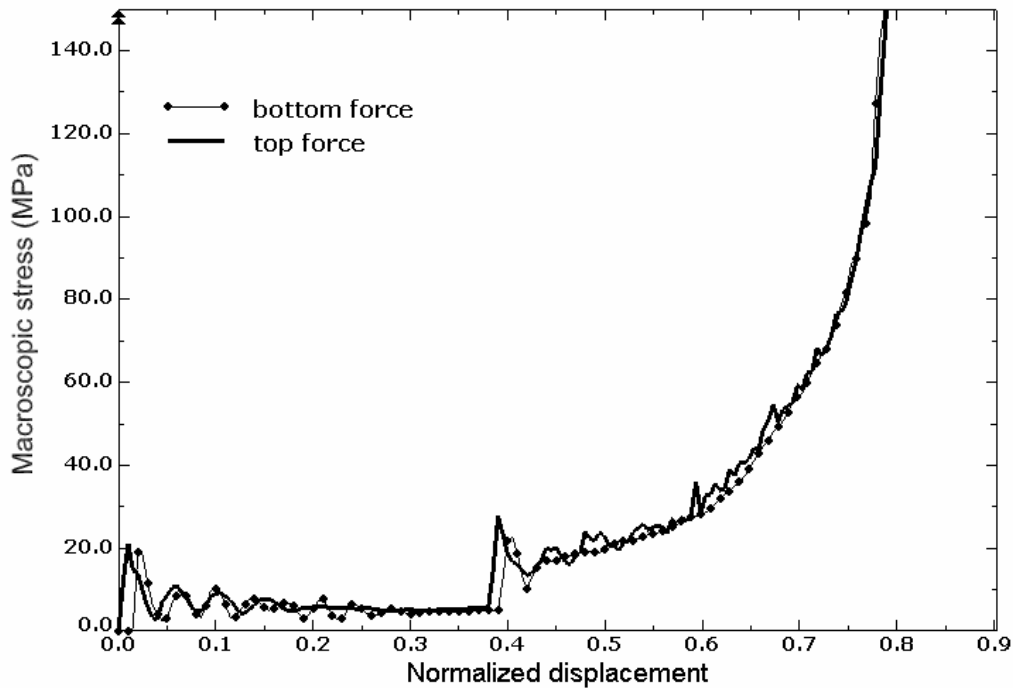


Figure 13: Macroscopic stress obtained with a velocity of 1.39 m/s

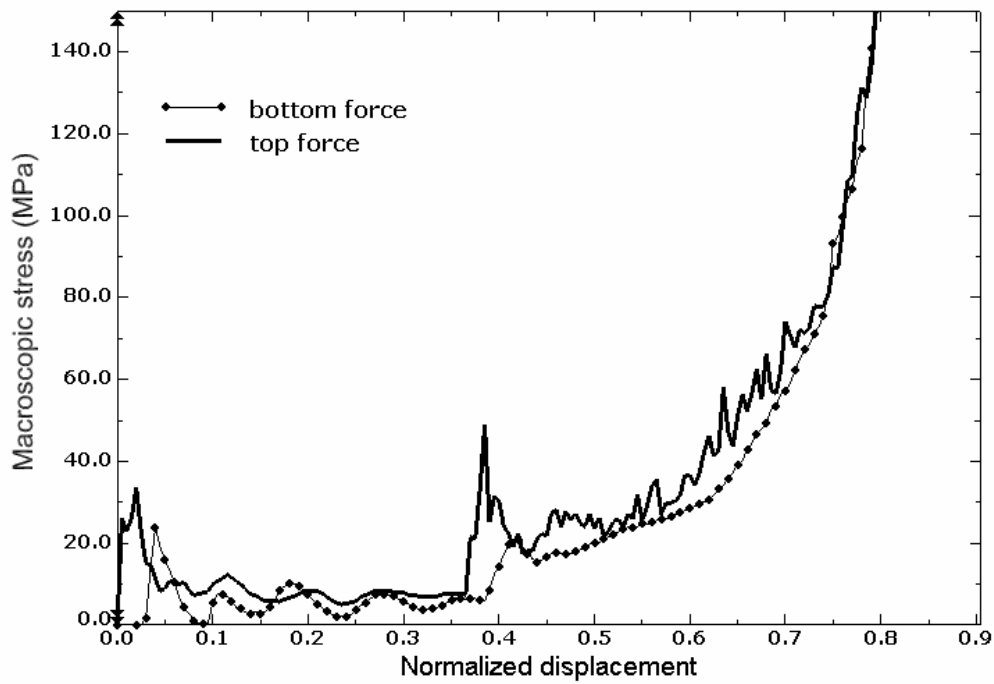


Figure 14: Macroscopic stress obtained with a velocity of 2.78 m/s

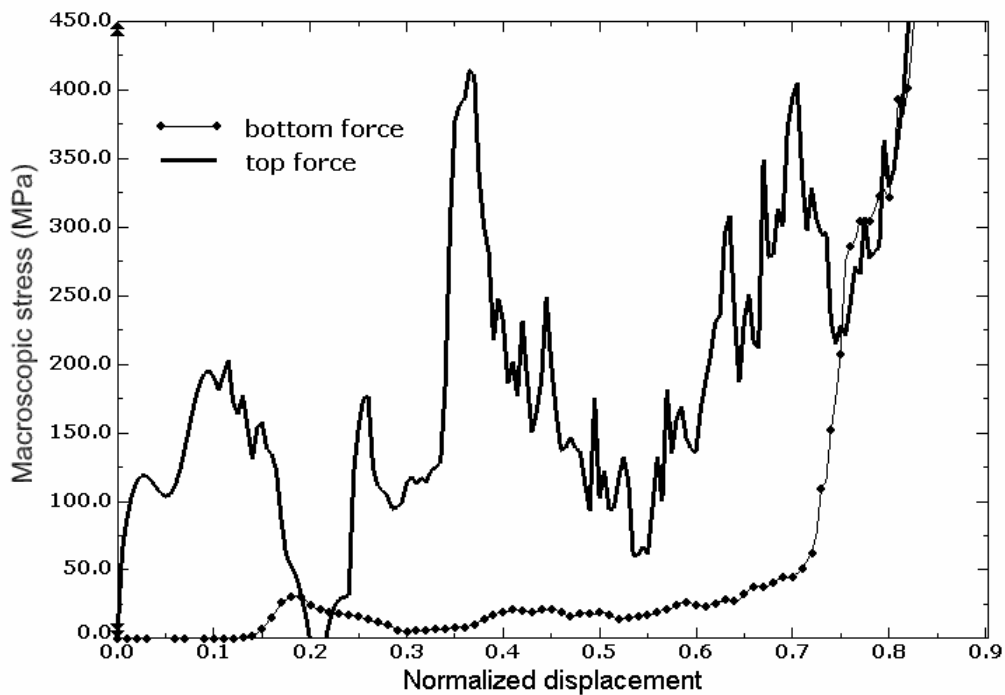


Figure 15: Macroscopic stress obtained with a velocity of 13.89 m/s

The differences between the top and bottom reactions are related to the propagation of the stress wave produced by the dynamic loading and are substantially reduced when the density assigned to the material is reduced, as shown in Fig. 16.

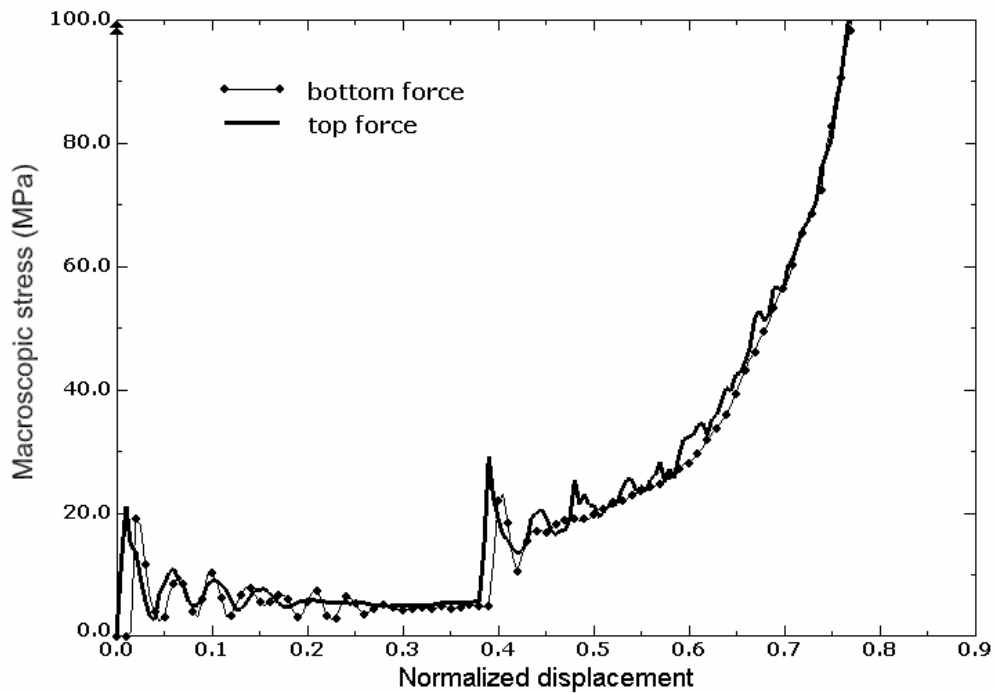


Figure 16: Reactions on top and bottom with a reduced density (1% from the original one) and a velocity of 13.89 m/s

The effect of the propagation of the stress wave may be seen also when analyzing a set of stacked cells, as indicated in Figs.17 and 18. For this geometry, an effect already noticed in an experimental research (Nemat-Nasser, 2007) is observed: under lower speeds, most of the plastic deformation takes place at the bottom cells, while at higher speeds, the cells at the top, in contact with the loading plane, are the most deformed.

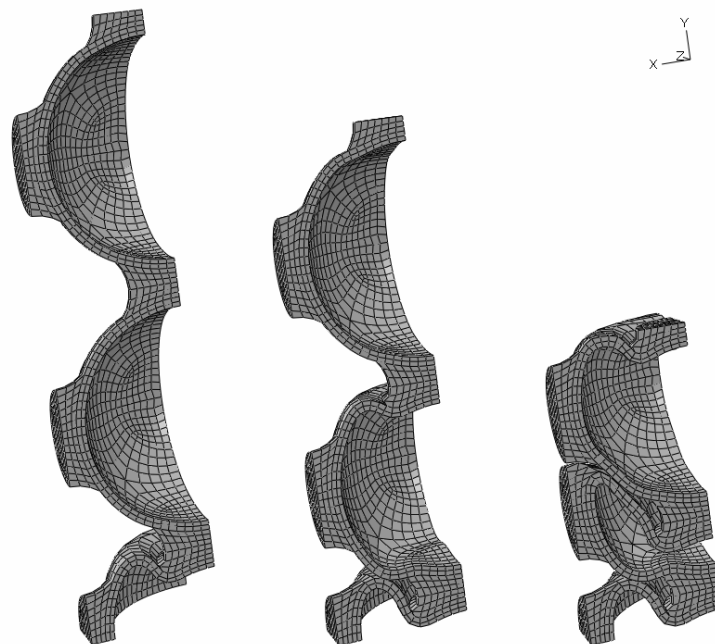


Figure 17: Deformation of a cells column at 10, 25 and 50% ratios of the target final normalized displacement, obtained with imposed loading velocity of 0.28 m/s

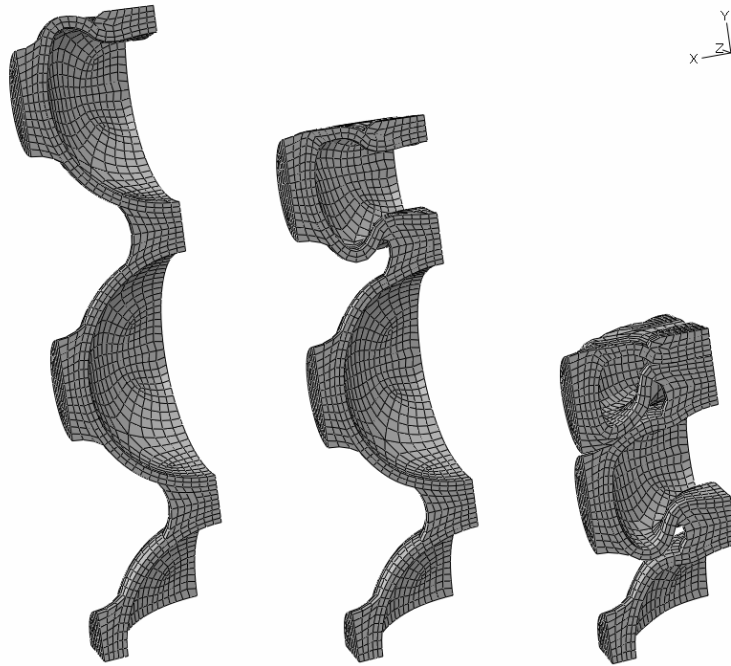


Figure 18: Deformation of a cells column at 10, 25 and 50% ratios of the target final normalized displacement, obtained with imposed loading velocity of 2.78 m/s

The influence of cell thickness (that determines inertia effects) is shown in Figs.19 to 21 for several rates of loading.

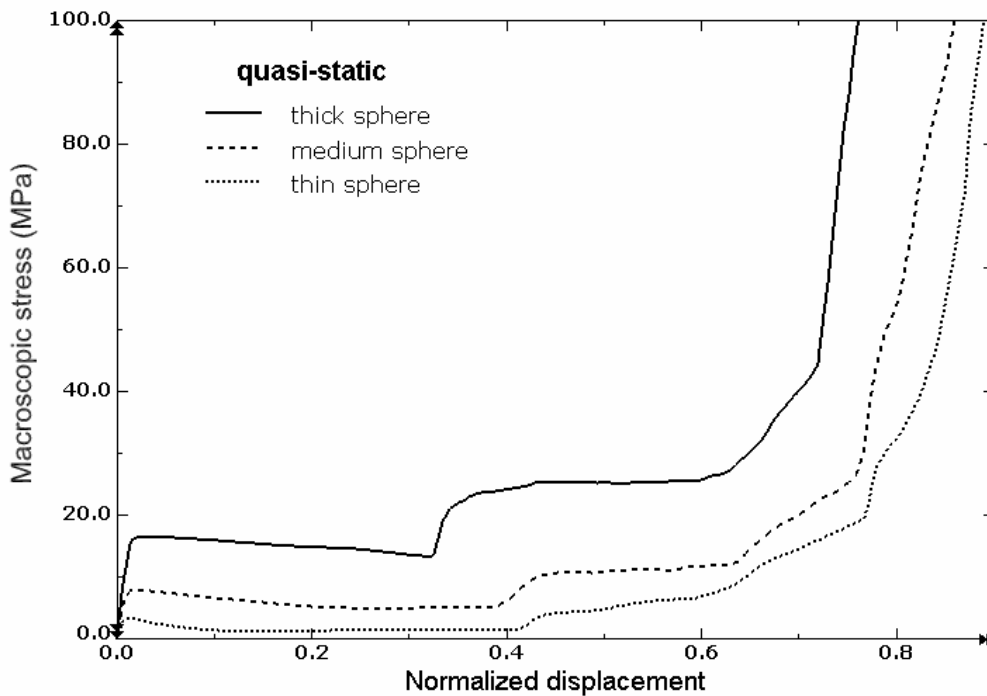


Figure 19: Macroscopic stress considering three thicknesses for a quasi-static analysis

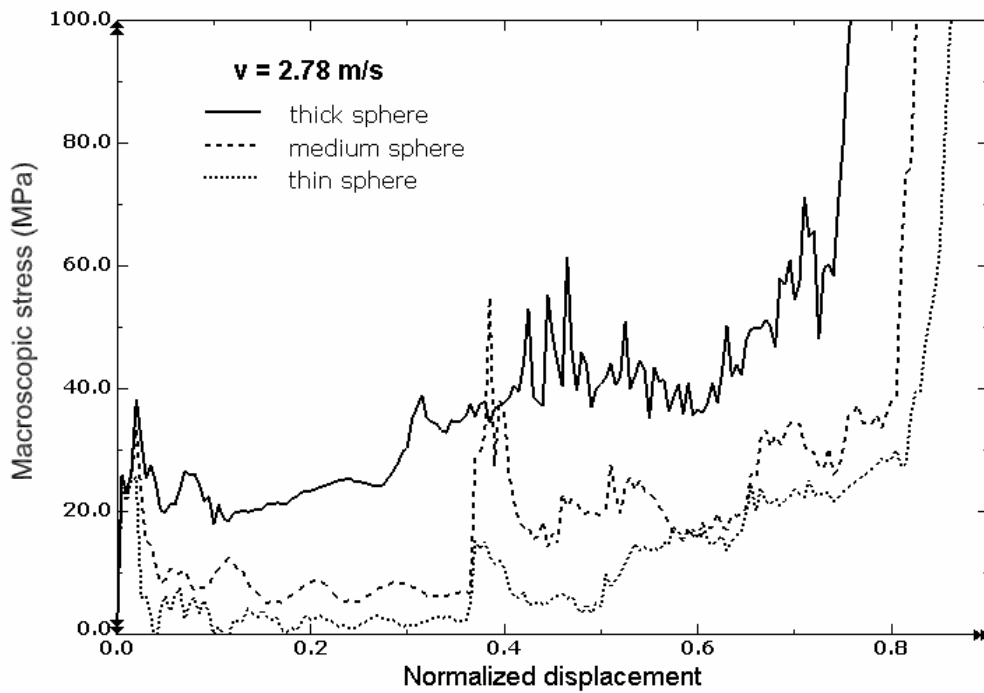


Figure 20: Macroscopic stress considering three thicknesses for a velocity of 2.78 m/s

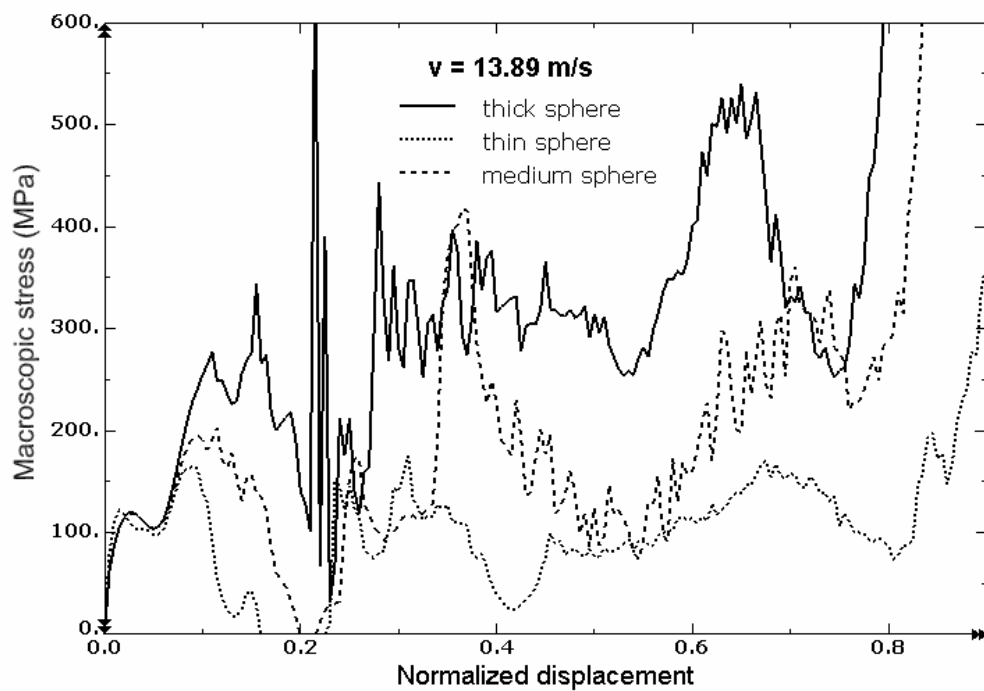


Figure 21: Macroscopic stress considering three thicknesses for a velocity of 13.89 m/s

Finally, Figs. 22 to 24 show the influence of base material strain-rate dependency.

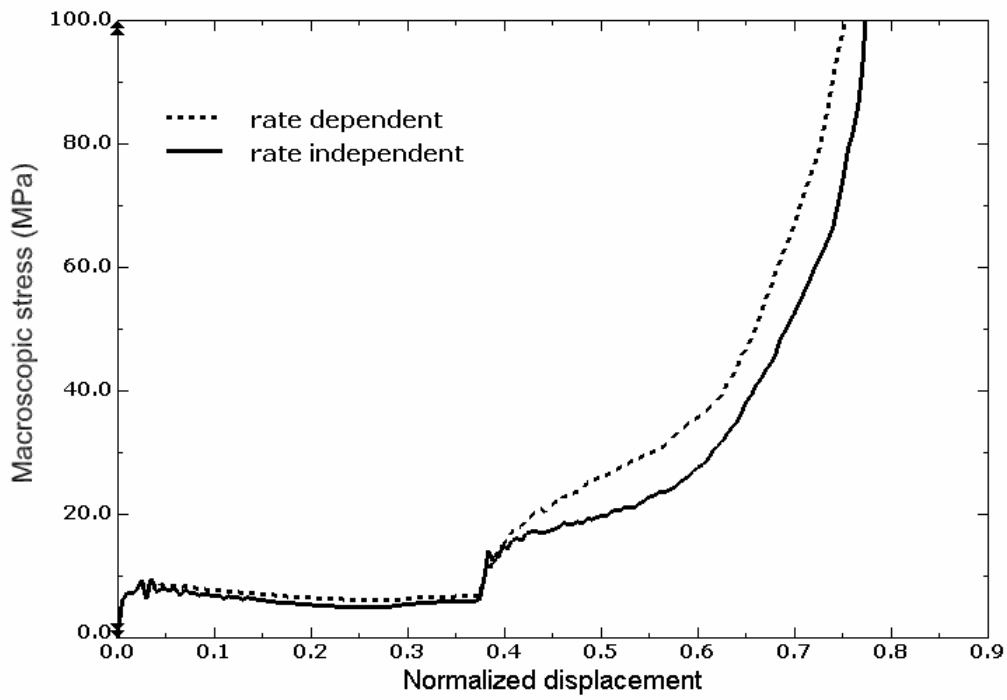


Figure 22: Macroscopic stress with and without rate dependence for a velocity of 0.28 m/s.

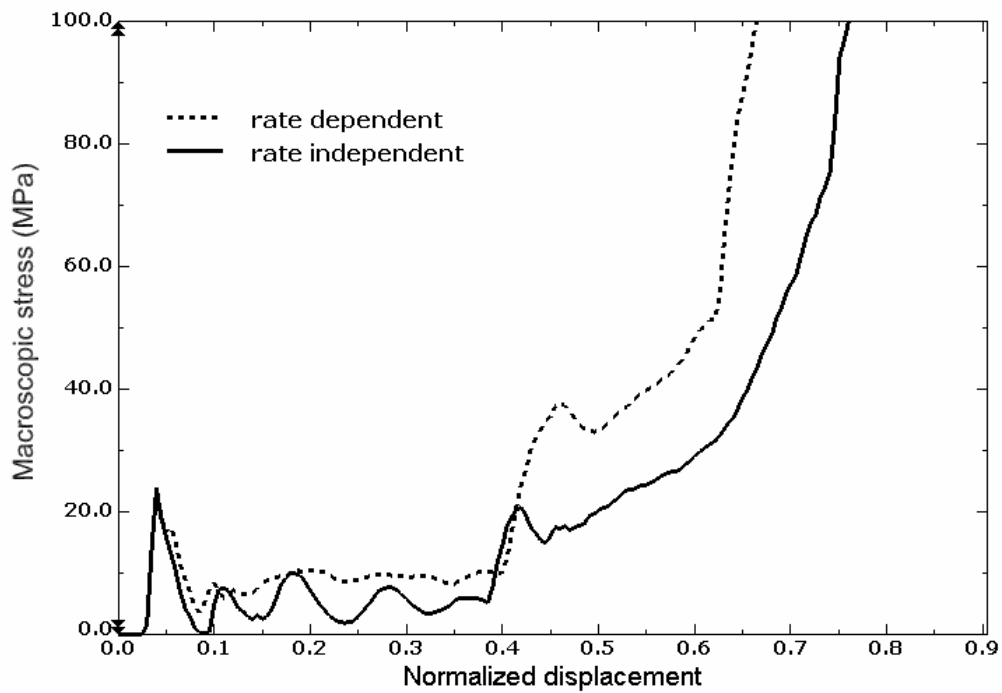


Figure 23: Macroscopic stress with and without rate dependence for a velocity of 2.78 m/s.

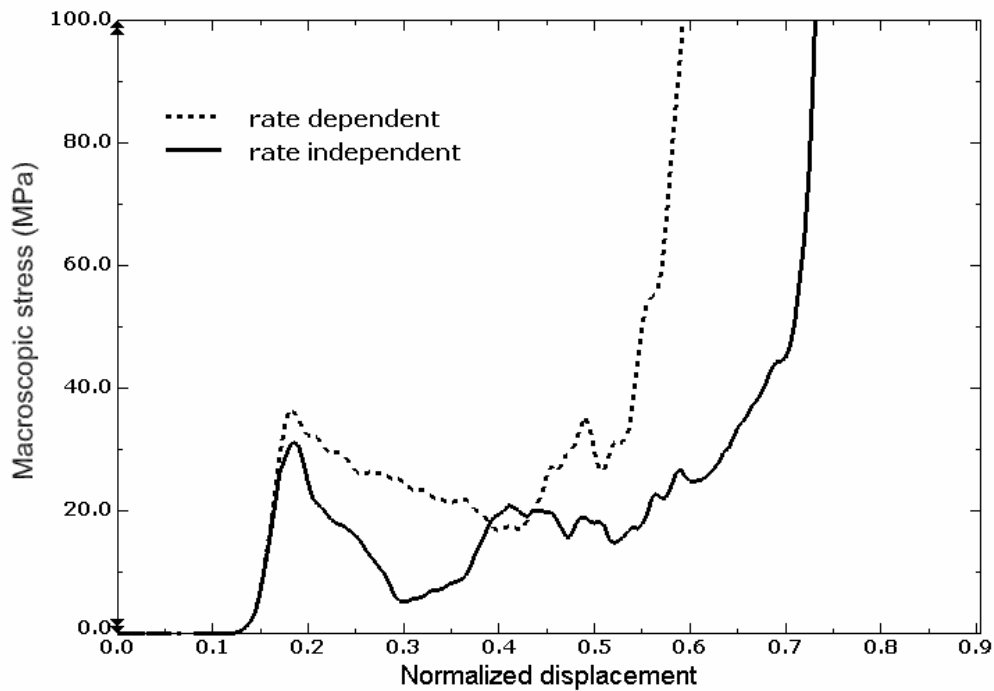


Figure 24: Macroscopic stress with and without rate dependence for a velocity of 13.89 m/s.

It can be observed that dynamic loading modifies the value and the localization of the peak load. The higher the velocity the higher are the peak stress and the normalized displacement value for its occurrence, as shown in Fig. 25.

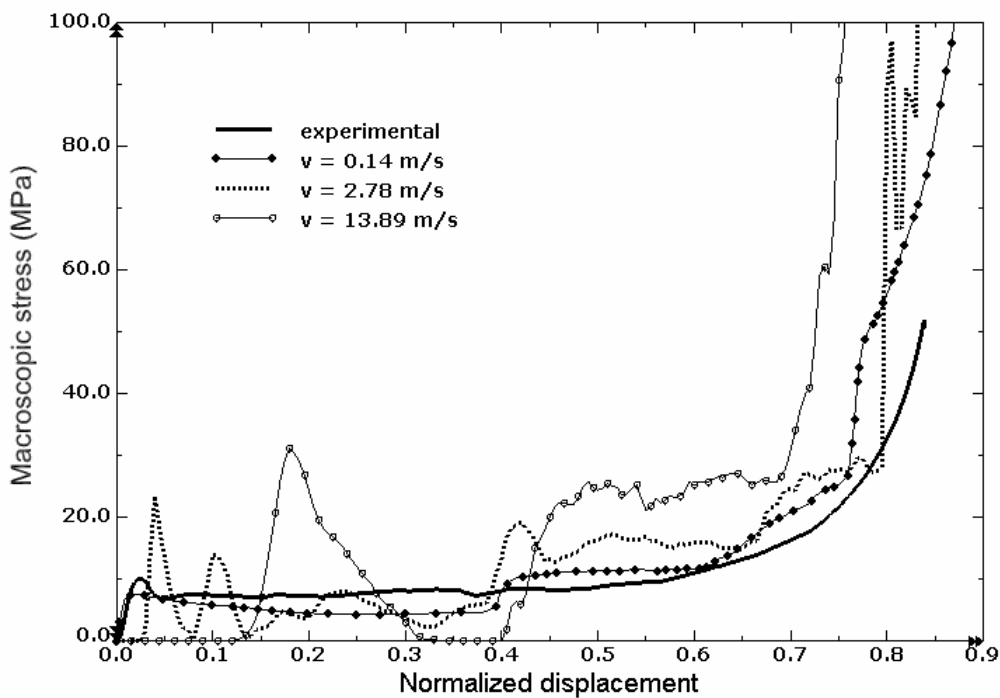


Figure 25: Macroscopic stress plots showing experimental and numerical results for the quasi-static case and numerical results for the dynamical analyses

Figures 26, 27 and 28 show the RVE deformed shapes at 25%, 50% and 75% of the normalized displacement for the different impact velocities analyzed. The propagation of the stress wave in the cells leads to higher concentrations of the stresses and plastic strains at the top of the cell (loaded region) with the growing velocities.

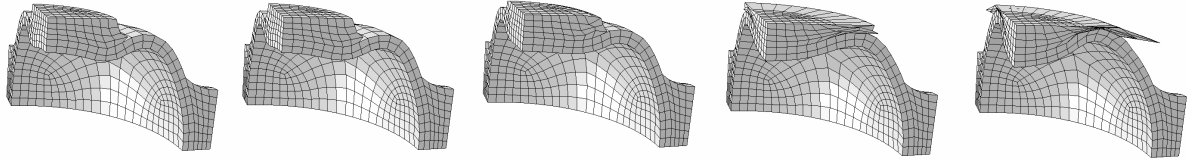


Figure 26: Deformed shapes at 25 % of the normalized displacement obtained with applied velocities of 0.14 m/s, 1.39 m/s, 2.78 m/s, 5.56 m/s and 13.89 m/s respectively from left to right

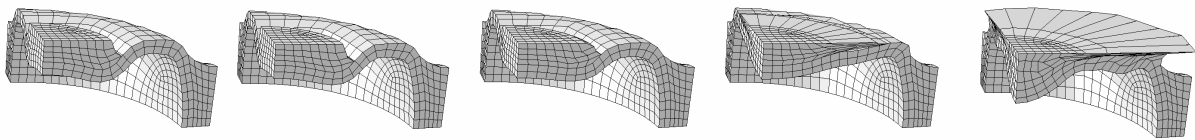


Figure 27: Deformed shapes at 50 % of the normalized displacement obtained with applied velocities of 0.14 m/s, 1.39 m/s, 2.78 m/s, 5.56 m/s and 13.89 m/s respectively from left to right

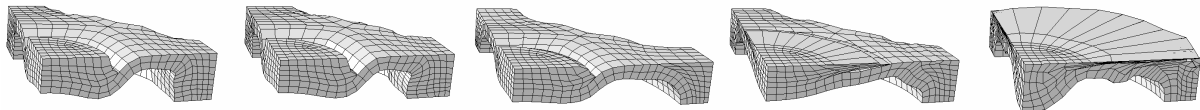


Figure 28: Deformed shapes at 75 % of the normalized displacement obtained with applied velocities of 0.14 m/s, 1.39 m/s, 2.78 m/s, 5.56 m/s and 13.89 m/s respectively from left to right

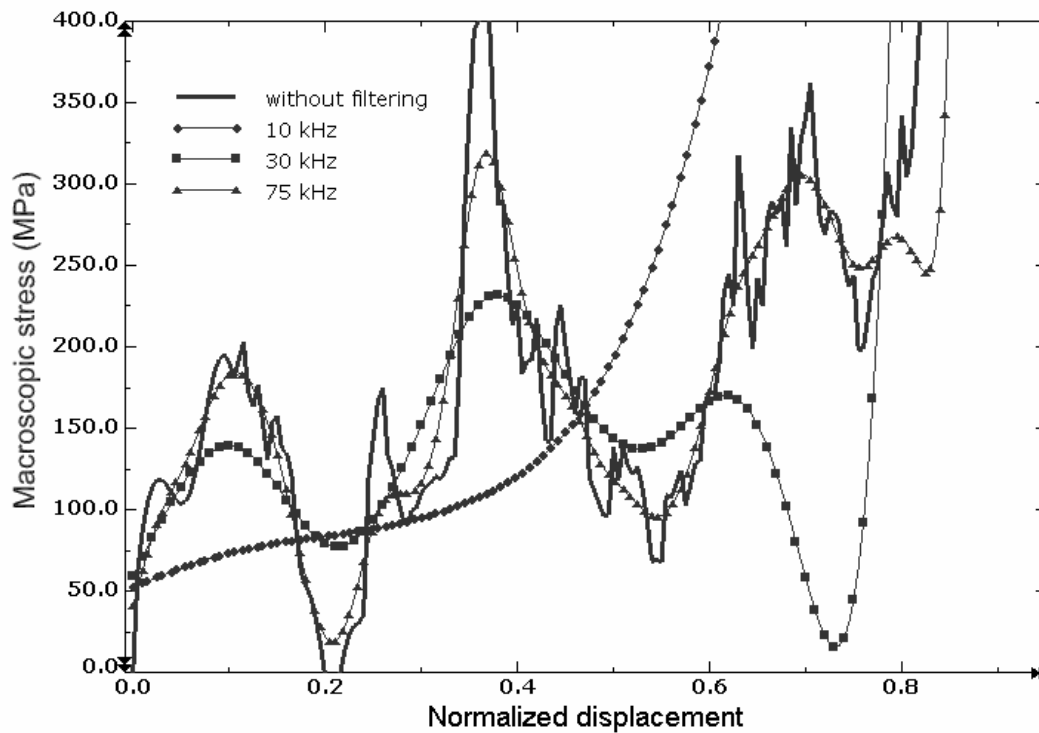


Figure 29: Macroscopic stresses evaluated from the top reaction using Butterworth filter with three different low cut-off frequencies.

Some of the oscillations that appear in the results corresponding to higher loading rates could be due to numerical effects, although similar oscillations are observed in experimental results (i.e. Fig. 10). In order to erase parasitic oscillations, numerical filters may be used. The results obtained through the use of these filters are, however, unwarranted, unless additional information (experimental results, for example) is available.

Figures 29 and 30 present macroscopic stresses evaluated considering the top reaction in a model compressed with a velocity of 13.89 m/s. The top reaction was filtered with the Butterworth filter available in Abaqus before to evaluate the macroscopic stresses. The filter was applied with different cut-off frequencies. The results presented in Fig. 29 shows that the filtering procedure applied with wrong parameters can lead to obviously erroneous results. If a higher cut-off frequency is employed, filtered results become closer to the unfiltered ones. In the present work, we choose to present the numerical results as given by ABAQUS, without the use of filters.

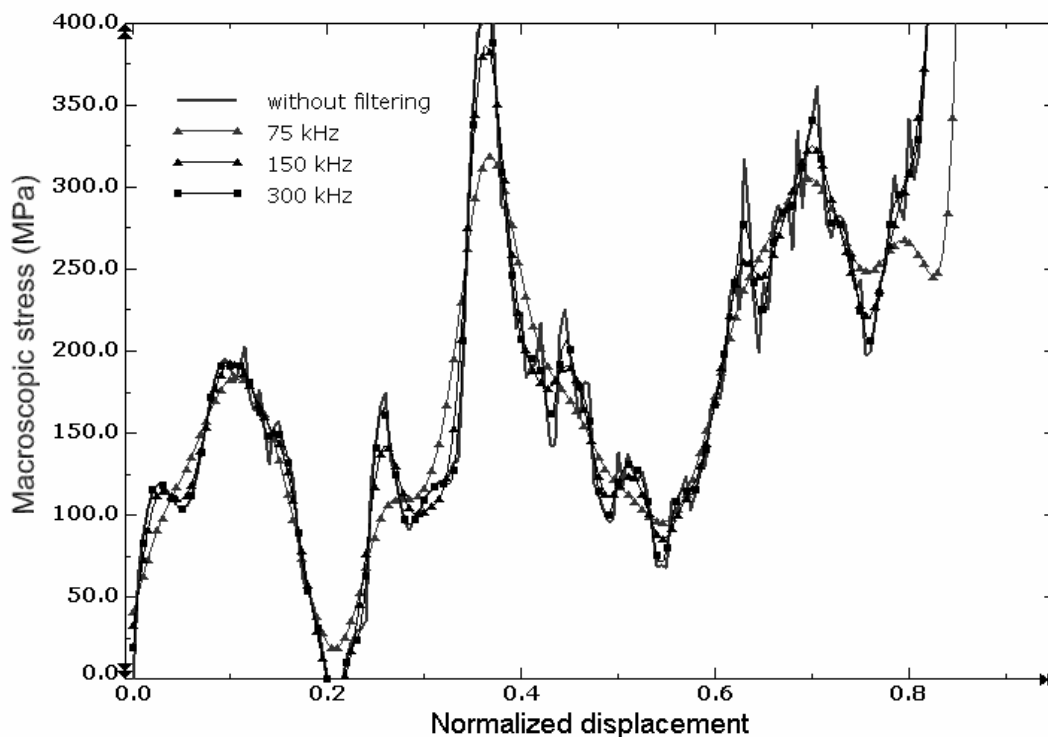


Figure 30: Macroscopic stresses evaluated from the top reaction using Butterworth filter with three different high cut-off frequencies.

5 CONCLUSIONS AND FINAL REMARKS

The load-deformation history of MHSS under different conditions of dynamical loading, including the effect of damage and rate-dependency was numerically determined. The Gurson model was used for damage and a power law model to introduce rate-dependency.

The results of the numerical examples presented show that both strain-rate and inertia play an important role in the dynamic behavior of this kind of energy-absorbing structures if the material of the structures is rate-sensitive, e.g. made of mild steel. When compared with the corresponding values in the quasi-static case, the combined effects of strain-rate and inertia make the peak load much higher. The effect of rate-dependency is more remarkable in higher velocities. In this case, the first peak load can be severely increased, and also the plateau stress level.

6 ACKNOWLEDGMENTS

The financial support of CNPq (Projects 572851/2008-1, 307787/2009-5, 480237/2007-7, 301068/2006-2), CAPES and PROPESQ-UFRGS are gratefully acknowledged. The authors thank the undergraduate students Fellipe Crós and Anderson Peccin da Silva for their collaboration in the numerical analyses.

REFERENCES

- Ashby, M.F., Evans, A., Fleck, N.A., Gibson, L.J., Hutchinson, J.W., and Wadley, H.N.G., *Metal Foams: A Design Guide*. Butterworth-Heinemann, 2000.
- Balch, D.K., O'Dwyer, J.G., Davis, G.R., Cady, C.M., Gray III, G.T., and Dunan, D.C., Plasticity and damage in aluminum syntactic foams deformed under dynamic and quasi-static conditions. *Materials Science and Engineering A*, 391:408-417, 2005.
- Cady, C.M., Gray III, G.T., Liu, C., Lovato, M.L., and Mukai, T., Compressive properties of a closed-cell aluminum form as a function of strain rate and temperature. *Materials Science and Engineering A*, 525:1-6, 2009.
- Calladine, C.R., and English, R. W., Strain-rate and inertia effects in the collapse of two types of energy-absorbing structure. *International Journal of Mechanical Sciences*, 26:689-701, 1984.
- Cardoso, E., and Oliveira, B.F., Study of the use of metallic foam in a vehicle for an energy-economy racing circuit. *Materialwissenschaft und Werkstofftechnik*, 41:257-264, 2010.
- Dannemann, K.A., and Lankford, J., High strain rate compression of closed-cell aluminium foams. *Material Science and Engineering A*, 293:157-164, 2000.
- Deshpande, V.S., and Fleck, N.A., High strain-rate compressive behaviour of aluminium alloy foams. *International Journal of Impact Engineering*, 24:277-298, 2000.
- Fiedler, T., *Numerical and Experimental Investigation of Hollow Sphere Structures in Sandwich Panels*. PhD thesis, University of Aveiro, Portugal, 2007.
- Gibson, L.J., and Ashby, M.F., *Cellular Solids, Structure and Properties*, 2 ed. Cambridge University Press, 1997.
- Gurson, A.L., Continuum theory of ductile rupture by void nucleation and growth. Part I. Yield criteria and flow rules for porous ductile media. *ASME Journal of Engineering Materials and Technology*, 99:2-15, 1977.
- Han, F.S., Cheng, H.F., Li, Z.B., and Wang, Q., The strain rate effect of an open cell aluminum foam. *Metallurgical and Materials Transactions A*, 36:645-650, 2005.
- Harrigan, J.J., Reid, S.R., and Seyed Yaghoubi, A., The correct analysis of shocks in a cellular material. *International Journal of Impact Engineering*, 37:918-927, 2010.
- Karagiozova, D., and Jones, N., Dynamic elastic-plastic buckling of cylindrical shells under axial impact. *International Journal of Solids and Structures*, 37:2005-2034, 2000.
- Koplik, J., and Needleman, A., Void growth and coalescence in porous plastic solids. *International Journal of Solids and Structures*, 24:835-853, 1988.
- Lee, S., Barthelat, F., Hutchinson, J.W., and Espinosa, H.D., Dynamic failure of metallic pyramidal truss core materials – experiments and modeling. *International Journal of Plasticity*, 22:2118-2145, 2006.
- Lindberg, H.E., *Little Book of Dynamic Buckling*. LCE Science/Software, 2003.
- Lindholm, U.S., Bessey, R.L., and Smith, G.V., Effect of strain rate on yield strength and elongation of three aluminum alloys. *Journal of Materials*, 6:119-133, 1971.
- Montanini, R., Measurement of strain rate sensitivity of aluminium foams for energy dissipation. *International Journal of Mechanical Sciences*, 47:26-42, 2005.

- Mukai, T., Miyoshi, T., Nakano, S., Somekawa, H., and Higashi, K., Compressive response of a closed-cell aluminum foam at high strain rates. *Scripta Materialia*, 54:533-537, 2006.
- Nemat-Nasser, S., Kang, W.J., McGee, J.D., Guo, W.G., and Isaacs, J., Experimental investigation of energy-absorption characteristics of components of sandwich structures. *International Journal of Impact Engineering*, 34:1119-1146, 2007.
- Öchsner, A., Winter, W., and Kuhn, G., On an elastic-plastic transition zone in cellular metals. *Archives of Applied Mechanics*, 73:261-269, 2003.
- Oliveira, B.F., Cunda, L.A.B., and Creus, G.J., Modeling of the mechanical behavior of metallic foams: damage effects at finite strains. *Mechanics of Advanced Materials and Structures*, 16:110-119, 2009a.
- Oliveira, B.F., Cunda, L.A.B., Öchsner, A., and Creus, G.J., Comparison between RVE and full mesh approaches for the simulation of compression tests on cellular metals. *Materialwissenschaft und Werkstofftechnik*, 39:133-138, 2008.
- Oliveira, B.F., Cunda, L.A.B., Öchsner, A., and Creus, G.J., Hollow sphere structures: a study of mechanical behaviour using numerical simulation. *Materialwissenschaft und Werkstofftechnik*, 40: 144-153, 2009b.
- Paul, A., and Ramamurty, U., Strain rate sensitivity of a closed-cell aluminium foam. *Materials Science and Engineering A*, 281:1-7, 2000.
- Reid, S.R., and Peng, C., Dynamic uniaxial crushing of wood. *International Journal of Impact Engineering*, 19:531-570, 1997.
- Su, X. Y., Yu, T. X., and Reid, S. R., Inertia-sensitive impact energy-absorbing structures, Part I: Effects of inertia and elasticity. *International Journal of Impact Engineering*, 16:651-672, 1995.
- Tam, L.L., and Calladine, C.R., Inertia and strain-rate effects in a simple plate-structure under impact loading. *International Journal of Impact Engineering*, 11:349-377, 1991.
- Tvergaard, V., Influence of voids on shear band instabilities under plane strain conditions. *International Journal of Fracture*, 17:389-407, 1981.
- Tvergaard, V., On localization in ductile materials containing spherical voids. *International Journal of Fracture*, 18:237-252, 1982.
- Zhao, H., Elnasri, I., and Abdennadher, S., An experimental study on the behaviour under impact loading of metallic cellular materials. *International Journal of Mechanical Sciences*, 47:757-774, 2005.